Assessment of long term pendulum and geodetic observations on a concrete arch dam

S. Gamse
Unit for Surveying and Geoinformation, Faculty of Engineering Science, University of Innsbruck, 6020 Innsbruck, Austria

M.J. Henriques
National Laboratory for Civil Engineering, Monitoring Devision, Av. do Brasil 101, 1700-066 Lisbon, Portugal

M. Oberguggenberger
Unit for Engineering Mathematics, Faculty of Engineering Science, University of Innsbruck, 6020 Innsbruck, Austria

Abstract. Long term measurements on dams expose the reversible deformations as a consequence of different loads on the object and above all irreversible deformations as a long term behavior of the structure. In our contribution the measurement data of an inverted pendulum and a geodetic traverse point in the same vertical line in/on a concrete arch dam are analyzed for a time period of 13 years. An optimal well-known hydrostatic-season-time model is estimated using a multiple linear regression for the data of the most top reading station of an inverted pendulum in the central cantilever of a concrete arch dam. The significant coefficients are defined using t-statistic of individual coefficient. The top models for radial and tangential displacements are also classified using Akaike and Bayes information criterion. After defining the most plausible model, displacements of the geodetic traverse point located on the dam crest, which are registered with lower measurement frequency as pendulum observations, are analyzed with the same HST-model.

Keywords. Concrete arch dam, geodetic observations, pendulum observations, hydrostatic-season-time model, multiple linear regression

1 Introduction

Large dams – embankment or concrete dams – are associated with important national and regional economic benefits. Most of the dams are still single-purpose dams, but there is a growing number of dams which are designed and constructed as multipurpose dams: irrigation, production of electricity, water supply, flood control, recreation, navigation, fish farming.

Due to the importance of dams and their potential risk in the case of any failure, public legislation regulates the safety control of large dams. Regulations are based on technical rules and procedures for the design, construction and monitoring of dams.

Structural safety control of dams is based on monitoring the behavior and performing the analysis of registered observations. The response of the dam due to the different and changeable influences (i.e. reservoir water level, temperature, aging, etc.) on the structure and its surrounding is observed by complementary monitoring methods. Displacement measurements involve different sensors such as pendulums, extensometers, inclinometers, rockmeters, fiber optic sensors, geodetic methods such as levelling, tacheometric observations and methods of Global Navigation Satellite Systems and additional sensors such as piezometers and thermometers. On concrete dams, the pendulum measurements and geodetic observations in traverse or triangulation networks are usually used for an assessment of planimetric displacements of different elements of the structure. The advantage of pendulum measurements is that they are more precise and can be easily included in an automatic monitoring system. The advantage of the geodetic methods is that they connect different parts of the dam (i.e. crest, abutments, and foundations), its surrounding area and even slopes and unstable rock

masses along the water reservoir, Rüger (2006). The geodetic observations are more expansive, therefore the measurement campaigns are less frequent, usually once or twice a year. In recent years, as a result of modern electronic and automatic tacheometers and a radical development on telecommunications, the importance of geodetic observations as a part of automatic and continuous monitoring systems is increasing.

For an assessment of measured values, captured by different sensors and methods, different analysis methods can be used. The main intention of the dam safety control is to compare the actual response of the structure, measured by different sensors, with the predictions of the estimated mathematical model, with the aim of an early detecting of anomalies and preventing failures, Salazar et al. (2015). The main influences on a concrete dam are the reservoir water level, temperature of water and air as reversible deformations and aging as irreversible deformations. The main three influences can be decomposed using a well-known statistical hydrostatic-season-time (HST) model.

In our contribution we analyzed the measurement data of Alqueva dam, a concrete arch dam. The measurement data at the most top reading station of a pendulum, which is installed in the central cantilever of the dam, are used to define the optimal HST-model. The unknown coefficients of the model are estimated using a multiple linear regression (MLR). Further, the differences between displacements of a geodetic point located on the dam crest and predicted radial and tangential values of the estimated HST-model at the same time epoch are analyzed.

2 Hydrostatic-Season-Time Model

The HST-model is a statistical/empirical model, which is based on the previous monitoring measurements of the dam behavior. It was first proposed in 1958 and has since been widely used for data analysis of concrete dams. Different models, which can be used for an analysis of the dam response to external forces, are described in Swiss Committee on Dams (2003).

For modelling of the water level influence, H_i, the polynomial function up to 4-th degree is used, Bonelli et al., 2016:

$$H_i = a_1 \cdot h_i + a_2 \cdot h_i^2 + a_3 \cdot h_i^3 + a_4 \cdot h_i^4 , \quad (1)$$

with a relative water level h_i:

$$h_i = \frac{h_{\max} - h(t_i)}{h_{\max} - h_{\min}} , \quad (2)$$

$h_{\max}$ maximal and $h_{\min}$ minimal water level in $[m]$ and $t_i : i = 0,1,2,..,N$ time step of observations.

The thermal effects, S_i, which expose seasonal variations, are modeled by a linear combination of sinusoidal functions, Swiss Committee on Dams (2003):

$$S_i = b_1 \cdot \sin(\omega_a \cdot t_i) + b_2 \cdot \cos(\omega_a \cdot t_i) + ...$$

$$... + b_3 \cdot \sin(2 \cdot \omega_a \cdot t_i) + b_4 \cdot \cos(2 \cdot \omega_a \cdot t_i) , \quad (3)$$

with an annual pulsation $\omega_a = 2\pi / \Delta t_a$ and $\Delta t_a = 365{,}25\ days$ for one year period with daily data.

For modeling of irreversible deformations as a consequence of a time influence, strictly monotone functions are proposed. In our computations, we used a linear term, a positive and a negative exponential function as suggested by Bonelli et al. (2016):

$$T_i = c_1 \cdot \tau_i + c_2 \cdot e^{\tau_i} + c_3 \cdot e^{-\tau_i} , \quad (4)$$

with reduced time τ_i during the analyzed period $[t_0, t_N]$, $\tau_i = (t_i - t_0)/(t_N - t_0)$.

The HST-model can be written for a time step t_i as:

$$y_i = a_0 + H_i + S_i + T_i + \varepsilon_i , \quad (5)$$

with a constant term a_0 and an error term ε_i (residuals), including measurement and modeling errors.

The unknown 12 parameters of the HST model can be estimated by a MLR. The most widely used technique of fitting the model to the data is the method of least squares, which minimizes the sum of residual squares,

$$\sum_{i=1}^{N} \varepsilon_i^2 \rightarrow \min , \quad (6)$$

where N is the size of measured data. We refer to Montgomery et al. (2012) for more details on linear regression analysis. The most difficult task or

challenge of the MLR is the selection of significant coefficients. In this process different methods can be used: backwards elimination, forward search or step-wise selection. In an iterative process, values of different statistical parameters are observed, such as multiple coefficient of determination, R^2, residual mean square error, MS_E, t-statistical test of significance of individual regression coefficients.

3 Data Description

In numerical evaluations, the monitoring data of the Alqueva dam, Figure 1, are processed. It is located on the Guadiana river and is designed as a multipurpose dam for irrigation, water supply, electric power generation and outdoor/touristic activities in Alentejo region, in south Portugal. The main structure is a concrete arch dam, with a maximum height of 96 m and a crest length of 458 m. Its hydrological basin has an area of 48,500 km^2. The dam was built between 1998 and 2002. The first filling of the reservoir begun in February 2002. In January 2010 the lake was filled to the planned level (full storage water level at an elevation 152 m, Figure 2), with a surface area of the reservoir of 250 km^2.

The installation of the monitoring equipment and the safety control of the main structure were carried out during the construction according to the monitoring plan - LNEC (1997). The plan includes the safety procedures to be followed during different periods of the dam maintenance, according to the Portuguese regulations – RSB (2007). The plan was complemented by different technical plans, including the one with requirements according to the geodetic monitoring of the dam LNEC (2000, 2001a, 2001b), Tavares de Castro and Henriques (2008).

For measuring planimetric displacements of the dam, eight pendulums were installed. Additionally, geodetic pillars, included in two traverse networks, were constructed on the dam.

3.1 Inverted Pendulum System and Geodetic Monitoring System

In Alqueva dam eight inverted pendulums, which have a fixed end at the lower point of the system (in the stiff rock beneath the structure), are installed. Absolute displacements of points at several reading stations located along the steel wire in inspection galleries are measured in radial (orthogonal to the downstream face of the block) and tangential (parallel to the downstream face) direction. The sensor readings are done manually; with weekly periodicity in the first years and reduced to one or two readings per month after the year 2005.

Fig. 1 Downstream face of Alqueva dam.
Source: https://en.wikipedia.org/wiki/Alqueva_Dam .

To control horizontal displacements, the geodetic monitoring system includes two traverse networks: one along the dam crest (height 154 m) and another in the horizontal inspection gallery number 4, (height 85 m). The points of the traverse network along the dam crest are materialized by concrete pillars with a forced centering. The geodetic campaigns were undertaken twice a year in the first years and once a year after 2006, Tavares de Castro and Henriques (2008).

In the paper, the measured data at the most top reading station of the pendulum FP4 installed in the central cantilever (middle of the dam) are analyzed.

The eight geodetic points (object points) of the traverse network along the dam crest are placed in a vertical line of each pendulum. In the paper, the geodetic point P4, located on the dam crest in a vertical line of the pendulum FP4 is analyzed. For geodetic observations of horizontal angles and distances, a motorized tacheometer TCA2003 Leica Geosystems, with an automatic target recognition, and precision prisms of the same manufacturer are used, Tavares de Castro and Henriques (2008).

Measured temperatures of the thermometer T64, installed at the level 141 m, in the middle of the central cantilever, between the highest and the second gallery, are plotted in Figure 3.

3.2 Statistical Analysis

In our work we performed following analyses:

- estimation of an optimal HST-model for planimetric – radial and tangential displacements at the most top reading station of the FP4 pendulum, situated in the highest gallery, at height 148 m;
- statistical evaluation of the model using coefficient of multiple determination R^2, residual mean square error, MS_E, t-statistic of individual coefficients, AIC and BIC information criterion;
- analysis of displacements of the geodetic point P4 on the dam crest, in the vertical profile of the pendulum FP4, using the estimated model.

The numerical and graphical results are given for both directions. In the radial direction, the hydrostatic load and the influence of water (and air) temperature, modeled with trigonometric functions, are more significant.

4 Analysis of Displacements

In the iterative process of defining the optimal HST-model for radial and tangential displacements on the pendulum data, we used backwards elimination. In the first step, all 12 coefficients are included. In further iterative procedure, the t-statistic of individual coefficients, Montgomery et al. (2012):

$$t_0 = \frac{\hat{\beta}_j}{\sqrt{\hat{\sigma}^2 \cdot C_{jj}}} \quad , \tag{7}$$

is used as a main criterion of an individual coefficient exclusion. If $|t_0| > t_{\alpha/2,N-k-1}$, the coefficient β_j is significant at significance level α and should be included into the model. k is a number of coefficients included in the model. Variance of the individual regression coefficient β_j is computed as: $V(\hat{\beta}_j) = \hat{\sigma}^2 \cdot C_{jj}$, with $C_{jj} = ((\mathbf{X}^T \cdot \mathbf{X})^{-1})_{jj}$, and $\hat{\sigma}$ calculated using equation (10). In the iterative procedure, further statistical parameters, such as multiple coefficient of determination, R^2, and residual mean square error, MS_E, and its root value were observed, which are not sufficient criteria for the model validation. The accuracy measures such as R^2 and $(R)MS_E$ always tend to the optimal model with

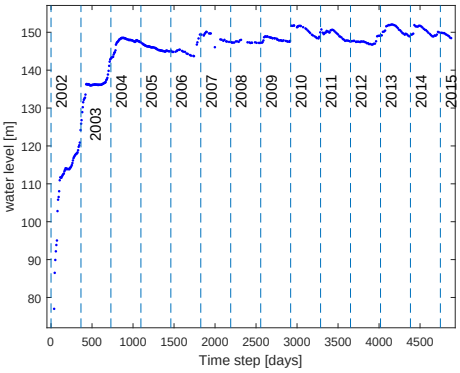

Fig. 2 Water level [m].

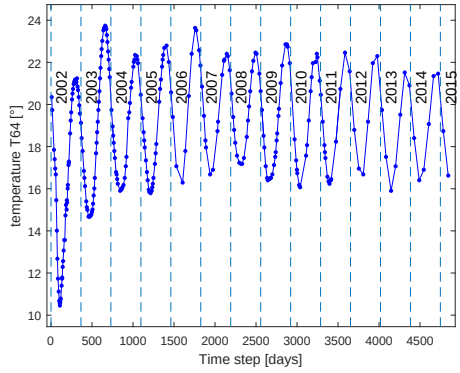

Fig. 3 Temperature at thermometer T64 [°].

more free parameters, which can lead to over-fitted model. In this case significant residuals or significant influences can be overlooked, because the identified model depends too much on the details of the data, and the noise in the data has an important role in the data fitting. An optimal model should fit the data well and remain sensitive/robust to outliers, i.e. measurement errors and modelled errors, Yuen (2010). The results of proposed optimal model are given in Table 1.

Additionally, all possible models, i.e. $2^{12-1}-1$, were classified according to Akaike (AIC) and Bayesian (BIC) information criterion, Yuen (2010):

$$AIC = \ln L - k \ , \tag{8}$$

$$BIC = \ln L - \frac{1}{2} \cdot k \cdot \ln k \ , \tag{9}$$

with the likelihood function L for the model. Both two criteria include an additional term, which penalizes complicated models, where the penalty

term is larger in BIC than in AIC.

The optimal model estimated by using the t-statistic of individual coefficients is the 1st top model for radial and 2nd top for tangential displacements according to AIC and BIC respectively. Exclusion of additional coefficients from the top models, selected using AIC and BIC, should be further analyzed by testing future predictions of the dam behavior.

Table 1. Parameters of proposed optimal HST-model for radial and tangential displacements for pendulum data

coefficient	radial	tangential
a_0	-28.89	10.74
a_1	97.30	-3.87
a_2	-231.69	-
a_3	140.99	15.10
a_4	-	-11.97
b_1	-8.42	-0.16
b_2	-3.33	-0.04
b_3	0.35	0.03
b_4	-0.54	-
c_1	-36.22	-20.42
c_2	11.69	5.99
c_3	-	-15.84
$RMS_E\ [mm]$	1.21	0.176
R^2	0.987	0.595

In Figure 4 and Figure 5 estimated parameters (blue dots) with standard deviations (brackets) and confidence intervals (red stars), computed for a 95%-confidence level, are plotted for radial and tangential displacement.

In Figure 6 and Figure 7 residuals of radial and tangential displacements with d and $2 \cdot d$ limit bound are plotted. The standard deviation of residuals converges to 1.2 mm for radial and to 0.2 mm for tangential direction. Residuals which are considerably larger in absolute value than the others indicate potential outliers. The limit bound d is usually a multiple of standard deviation $\hat{\sigma}$, computed for some reference period as, Swiss Committee on Dams (2003):

$$\hat{\sigma} = \sqrt{(\varepsilon_1^2 + \varepsilon_2^2 + ... + \varepsilon_N^2)/(N-k-1)}\ . \quad (10)$$

The computed d-bounds are 1.2 mm and to 0.2 mm for radial and tangential direction. In both directions there are residuals, which can expose outliers. On average, the residuals confirm a good coincidence of the proposed estimated model with the measured data.

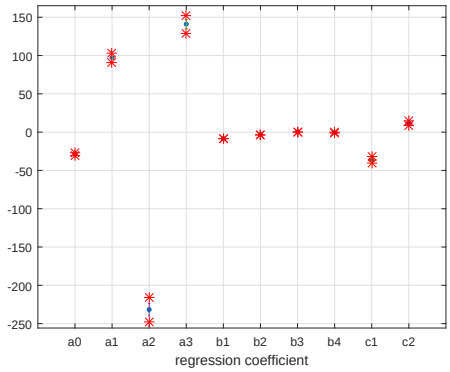

Fig. 4 Estimated parameters (blue dots), standard deviations (brackets) and confidence intervals (red stars): radial displacements.

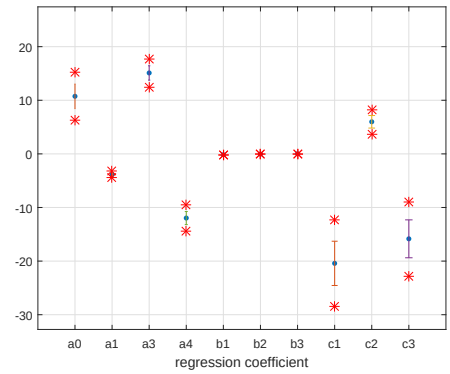

Fig.5 Estimated parameters (blue dots), standard deviations (brackets) and confidence intervals (red stars): tangential displacements.

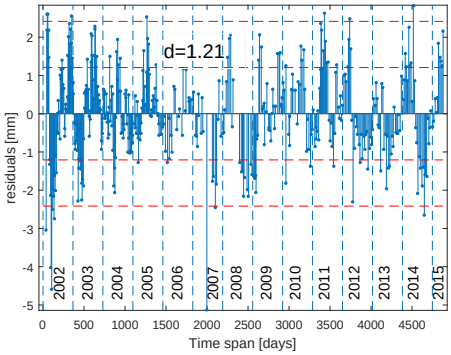

Fig. 6 Residuals (blue bars/dots) with d and $2 \cdot d$ limit bound (red dashed lines): radial displacements.

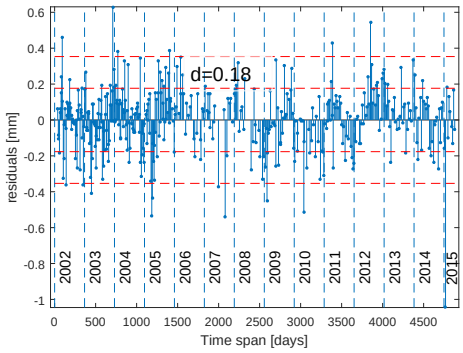

Fig. 7 Residuals (blue bars/dots) with d and $2 \cdot d$ limit bound (red dashed lines): tangential displacements.

With the proposed optimal HST-model, the decomposed influences – hydrostatic, temperature and time influence can be computed. They are plotted in Figure 8 and Figure 9.

The displacements, measured with the pendulum at the most top reading station, were compared with displacements of the geodetic pillar on the dam crest. With the proposed optimal HST-model, the predicted values of radial and tangential displacements were computed for the time epochs of geodetic campaigns. The frequency of geodetic observations in the first years was twice a year and since 2006 reduced to once a year. The reduced number of geodetic campaigns carried out until May 2015 does not enable the computation of the HST-model for the measured displacements of the geodetic pillar. Therefor the differences were analyzed with the HST-model estimated for pendulum data. The differences are plotted in Figure 10 and Figure 11 and amounts up to 8 mm in radial and 1 mm in tangential direction.

In Figure 12 and Figure 13, the results are presented graphically. For each direction, radial and tangential displacements, the predicted values, computed with the proposed optimal HST-model with the 95%-confidence interval, measured values, captured with a pendulum and with geodetic measurements in a traverse network, are plotted.

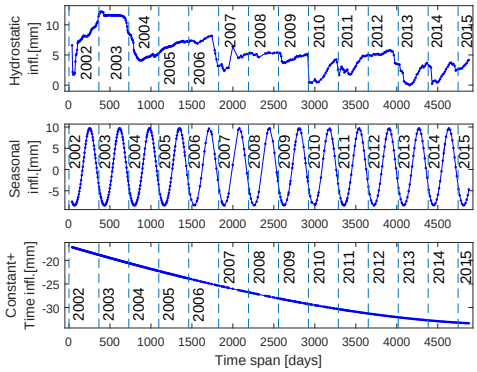

Fig. 8 Estimated hydrostatic (top), temperature (middle) and time (bottom) influence: radial displacements.

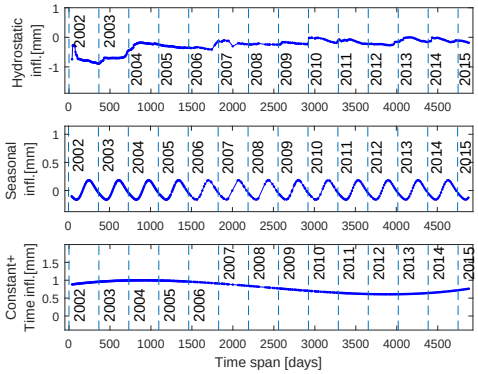

Fig. 9 Estimated hydrostatic (top), temperature (middle) and time (bottom) influence: tangential displacements.

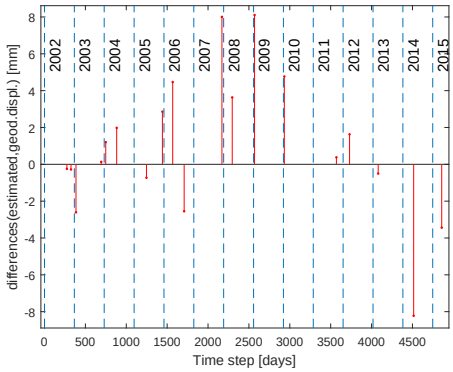

Fig. 10 Differences between predicted displacements, computed with proposed optimal HST-model, and measured displacements of geodetic point: radial displacements.

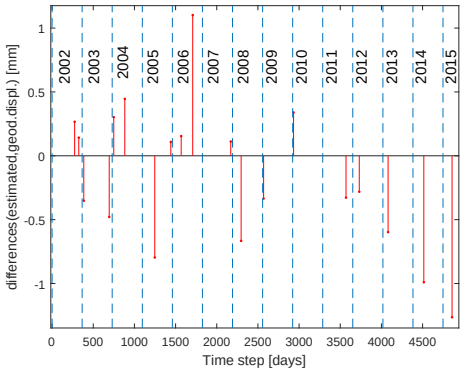

Fig. 11 Differences between predicted displacements, computed with proposed optimal HST-model, and measured displacements of geodetic point: tangential displacements.

5 Conclusions

One of the main intentions of the work is to compare displacements, measured by geodetic methods, with the pendulum data.

For the pendulum data (displacements in radial and tangential direction measured at the most top reading station), the optimal HST-model is computed using MLR and t-statistic as the main criterion for the coefficient exclusion. For both directions, the proposed optimal models include 10 coefficients. For further exclusion of coefficients, as proposed/computed for top-models using AIC and BIC criterion, further validations should be done, especially tests on future predicted displacements.

The coincidence of the displacement captured with the pendulum and geodetic measurements is in the range of 1 mm in tangential direction and less than 1 cm in radial direction. In tangential direction there are differences with the same sign and increasing values since 2012.

The possible correlations of displacement differences and displacements, measured with geodetic observations, with the air temperature could be analyzed. Possible reason for bigger differences in radial direction can be due to a fact that the geodetic pillar (at elevation 154 m) is 6 m above the first inspection gallery (at elevation 148 m), where the most top reading station of each pendulum is located.

The same analysis could be done for other pendulum data and geodetic pillars on the dam crest.

In future work the hydrostatic-temperature-time model, as proposed in Mata et al. (2014), could be implemented.

References

Bonelli, S., R. Tourment, H. Felix (accessed on 2016). Analysis of earthdam monitoring data. Cemagref, France. https://www.researchgate.net/publication/228744938_Analysis_of_earthdam_monitoring_data (accessed on 5.1.2016).

LNEC (1997). Observation plan of Alqueva scheme. Dam, foundation, surrounding rock mass, reservoir and appurtenant works (in Portuguese). *Internal report, LNEC, Lisbon.*

LNEC (2000). Alqueva Scheme: Preliminary Plan of the Geodetic Observation System (in Portuguese). *Internal report, LNEC, Lisbon.*

LNEC (2001a). Alqueva Scheme: Note on the Geodetic Observation System. (in Portuguese). *Internal report, LNEC, Lisbon.*

LNEC (2001b). Alqueva Scheme: The Precision Traverse on the Crest of the Dam. (in Portuguese). *Internal report, LNEC, Lisbon.*

Mata, J., A.T. de Castro, J.S. da Costa (2014). Constructing Statistical Models for Arch Dam Deformation. *Structural Control and Health Monitoring*, 21, pp. 423-437. Doi: 10.1002/stc.1575.

Montgomery, D.C, E.A. Peck, G.G. Vining (2012). Introduction to linear regression analysis. John Wiley & Sons, Inc.

RSB (2007). Regulation for safety of dams. (in Portuguese). *Decree-law n.º 344/2007*.

Rüger, J.M. (2006). Overview of Geodetic Deformation Measurements of Dams. ANCOLD Conference. Nov. 19-22, 2006. Manly, Sydney. Available online http://www.gmat.unsw.edu.au/snap/publications/rueger 2006a.pdf (accessed on 12.10.2014).

Salazar, F., M.A. Toledo, E. Onate, R. Morán (2015). An Empirical Comparison of Machine Learning Techniques for Dam Behaviour Modelling. *Structural Safety*, 56, pp. 9-17. Doi: 10.1016/j.strusafe.2015.05.001.

Swiss Committee on Dams (2003). Arbeitsgruppe Numerische Methoden in der Analyse des Verhaltens von Talsperren. *Analysemethoden für die Vorhersage und Kontrolle des Verhaltens von Talsperren*. http://www.swissdams.ch/index.php/de/ (accessed on 15.6.2015).

Tavares de Castro, A., M.J. Henriques (2008). Monitoring planimetric displacements in concrete dams. 13-th FIG Symposium on Deformation Measurement and Analysis. LNEC, May 12-15, 2008. Lisbon, Portugal.

Yuen, K. (2010). Bayesian methods for structural dynamics and civil engineering. John Wiley & Sons (Asia) Pte Ltd.

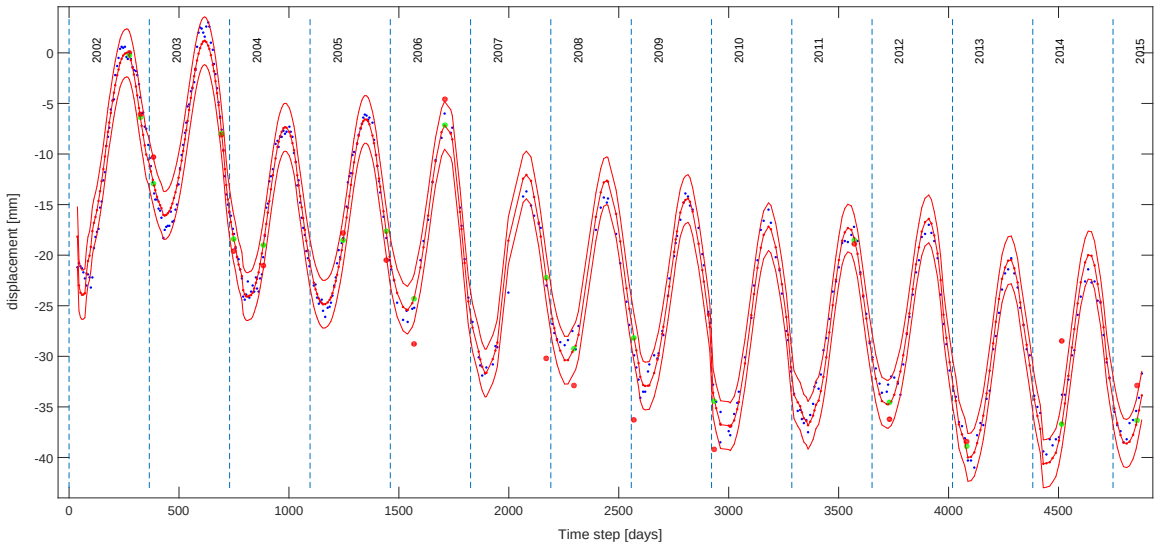

Fig. 12 Estimated (red line with dots), measured (blue dots) pendulum values, 95% -confidence bound, displacements of geodetic pillar – measured (big red dots) and estimated (big green dots): radial displacements.

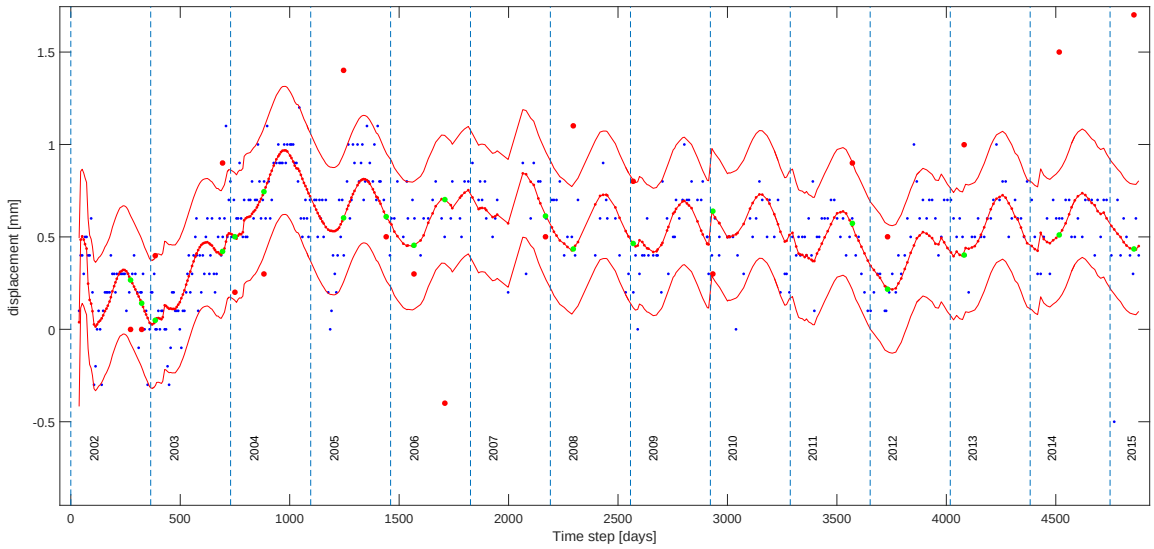

Fig. 13 Estimated (red line with dots), measured (blue dots) pendulum values, 95% -confidence bound, displacements of geodetic pillar – measured (big red dots) and estimated (big green dots): tangential displacements.